Steady-State Process Optimization with Guaranteed Robust Stability and Feasibility

M. Mönnigmann and W. Marquardt
RWTH Aachen University, D-52056 Aachen, Germany

A new approach is presented to the optimization based design of continuous processes in the presence of parametric uncertainty. In contrast to previous works focusing on process feasibility, it allows to consider both feasibility and stability of the process in the presence of parametric uncertainty. The new approach, therefore, permits an integrated treatment of steady-state flexibility and robust stability in the optimization of continuous processes. The process optimization problem is extended by constraints that ensure a lower bound on the distance of the nominal point of operation to stability and feasibility boundaries in the space of the uncertain parameters. While previous approaches are based on evaluating constraint violation in the range space of the constraints, the measure for flexibility and robustness used here is given in the domain space of the uncertain parameters. The method is discussed in the context of existing approaches to flexibility in process optimization and is illustrated with a continuous polymerization which is known to have a nontrivial stability boundary resulting from multiple steady states and sustained oscillations.

Introduction

Models of chemical engineering processes are subject to inaccuracy and uncertainty. Numerous articles have addressed the problem of process design under uncertainty over the past two decades. Grossmann and coworkers (Swaney and Grossmann 1985; Halemane and Grossmann, 1982) introduced feasibility and flexibility measures on which many later articles are based. These measures allow (1) to determine if a given design is feasible despite the presence of parametric uncertainty, (2) to calculate a scalar index of design flexibility, which, for example, allows to compare different designs, and (3) to identify bottlenecks which impede the desired flexibility. Several approaches have been suggested to solve the optimization problems that arise in determining the proposed flexibility and feasibility measures. Early approaches had to assume that global optima occur at vertices of a hyperrectangle of uncertain parameters (Swaney and Grossmann, 1985). Later research was devoted to relaxing this assumption (Grossmann and Floudas, 1987; Ostrovsky et al., 2000; Kabatek and Swaney, 1992). A more recent approach is based on branch and bound global optimization (Floudas et al., 2001).

The development of *process flexibility measures* is still subject to research. Ierapetritou (2001) presented a new approach to analyzing the feasible region of 1-D (one-dimensional) quasi-convex problems, which provides a more accurate description of the true feasible space than previous methods. The approach is based on determining the convex hull of a set of points on the boundary of the feasible region. These points are determined from optimization problems similar to the ones proposed by Swaney and Grossmann (1985).

Based on the flexibility and feasibility measures, methods for *process optimization under uncertainty* have been developed. Bahri et al. (1996) presented a two-level optimization procedure for the optimization-based design of continuous processes in the presence of uncertainty at steady state. The authors evaluate design flexibility and detect critical values of the uncertain parameters based on constraint violation in the range space of the constraints, similar to the measures proposed by Grossmann and coworkers (Halemane and Grossmann, 1982; Swaney and Grossmann, 1985). Bahri et al. (1997)

Correspondence concerning this article should be addressed to W. Marquardt.

discuss the extension of this approach to dynamic process systems.

Mohideen et al. (1996) introduce an iterative procedure for optimization-based design in the presence of uncertainty that is based on an *active set strategy* (Grossmann and Floudas, 1987). The approach makes use of the feasibility and flexibility measures introduced by Grossmann and coworkers. An extension of these measures to dynamic disturbances has later been suggested (Dimitriadis and Pistikopoulos, 1995). Dynamic disturbances are incorporated into the design process in the form of scenarios to allow for the treatment of flexibility and controllability. In a successive work Mohideen et al. (1997) augment their procedure by eigenvalue bounds based on matrix measures (Kokossis and Floudas, 1994) in order to avoid flexible and optimal, but unstable designs.

Bansal et al. (2001) outline a method based on *parametric programming*. This approach allows to determine explicit expressions for the feasibility and flexibility measures as functions of the uncertain parameters *a priori* to the actual process design step. These explicit expressions predict in which regions of the process parameter space feasible operation can be guaranteed despite uncertainty. Once obtained, the explicit feasibility and flexibility functions can be used to find an optimal flexible process design. This approach in particular avoids two-level or nested optimizations as employed in the methods mentioned so far. Algorithms for the solution of single- and multiparametric MILPs (Acevedo and Pistikopoulos, 1997; Bansal et al., 2000), and convex MINLPs where uncertain parameters enter linearly (Papalexandri and Dimkou, 1998; Pertsinidis et al., 1998) and their application to process design problems under uncertainty have been presented. Both parametric programming-based design methods and the approach presented here avoid iterations of optimization problems which arise because of the max-min-max definitions of feasibility and flexibility measures (Halemane and Grossmann, 1982; Swaney and Grossmann, 1985).

Luyben and Floudas (1994) treat controllability and economic profit as distinct objectives in a *multiobjective optimization* approach. In this approach, open-loop controllability enters the optimization problem in the form of controllability indices for a linear approximation of the process at an operating point. While not addressed by Luyben and Floudas (1994), the authors point out that flexibility and uncertainty may be treated by considering them in additional design objectives in their multiobjective optimization approach.

Much work has addressed the question of *how to describe parametric uncertainty* correctly and with sufficient precision. For applications in which a more precise description is too expensive or tedious to obtain, hyperrectangular uncertainty regions are often used (see, for example, Mohideen et al., 1996, 1997; Bahri et al., 1996, 1997). A more precise descriptions can, however, be incorporated into the design procedures. Pistikopoulos (1995) discusses the problem of design under stochastic uncertainty and the concept of information cost. The impact of the precision of the description of parametric uncertainty on the design has been investigated by Rooney and Biegler who compare hyperrectangular uncertainty regions to elliptical joint confidence regions (Rooney and Biegler, 1999) and to confidence regions derived from the likelihood ratio test (Rooney and Biegler, 2001). They show that these more precise approaches greatly improve the description of uncertainty in the examples presented, and they incorporate them into an existing algorithm (Grossmann and Floudas, 1987) for design under uncertainty.

This article addresses the steady-state optimization of continuous processes that are subject to parametric uncertainty. The major contribution of this work is a unified description of the feasibility and stability boundaries, and the derivation of constraints for parametric robustness based on this description. While approaches for guaranteeing *feasibility* in the presence of parametric uncertainty have been established in previous work, an equally general approach to ensuring process *stability* under parametric uncertainty does not exist to the authors' knowledge. This is the more surprising as problems related to a loss of stability of optimal process designs have been encountered in applications of existing approaches to optimization-based design some time ago (Kokossis and Floudas, 1994; Mohideen et al., 1997). Roughly speaking, a unified treatment of both feasibility and stability boundaries is possible if the notion of *constraint violation* in the sense of Grossmann and coworkers (Halemane and Grossmann, 1982; Swaney and Grossmann, 1985) is replaced by evaluating process designs according to their *distance to critical boundaries in the space of the uncertain parameters*. We call attention to the fact that measuring constraint violation amounts to evaluating designs in the range space of the feasibility constraints. In contrast, the approach suggested here assesses process designs by measuring distances in the space of the uncertain parameters, that is, by a measure which is given directly in the domain of the uncertain process parameters. This detail, which seems quite technical at first sight, in fact allows to treat both stability and feasibility in a unified manner.

While the examples in this article are limited to open-loop systems, the proposed method can be applied to closed-loop systems without modifications. This will be detailed in the next section. For a small example of a closed-loop system, see Mönnigmann and Marquardt (2002b).

The next section states the problem class which is addressed. It is followed by a sketch of the solution approach. This sketch introduces the notion of critical boundaries, and it explains how this idea applies both to feasibility constraints and stability in process optimization. After having outlined the intuitive ideas, the section entitled *Normal spaces to manifolds* introduces the terminology which is necessary in the subsequent section to state the constraints for parametric robustness with respect to feasibility and stability. The conceptual part of the article closes with the statement of the formal nonlinear program with constraints for robustness. Throughout the conceptual part, a simple fermenter model is used for illustrative purposes. Results of the application of the proposed approach to a more complex example, a polymerization reaction carried out in a continuous stirred tank reactor (CSTR), are then reported in a subsequent section. Finally, a summary and a brief outlook are given.

A First Problem Formulation

In this article nonlinear dynamical systems are addressed that can be modeled in terms of ordinary differential equations and algebraic equations. We start with a general nonlinear systems notation. This notation allows us to point out

that our approach can be applied to both open-loop and closed-loop systems. In addition, this notation allows us to state the requirements that must hold for an application of our approach. Once the requirements have been stated, we will introduce a strongly simplified notation which is natural for the normal vector constraints on which the presented approach is based.

A broad class of nonlinear systems can be modeled by equations of the form

$$\begin{aligned} \dot{x}^d(t) &= f^d\left(x^d(t), x^a(t), u(t), d(t), \vartheta, t\right), \quad x^d(0) = x_0^d, \\ 0 &= f^a\left(x^d(t), x^a(t), u(t), d(t), \vartheta, t\right), \\ y(t) &= h\left(x^d(t), x^a(t), u(t), d(t), \vartheta, t\right) \end{aligned} \tag{1}$$

where $x = (x^{dT} x^{aT})^T \in \mathbb{R}^{n_x}$, $u \in \mathbb{R}^{n_u}$, $d \in \mathbb{R}^{n_d}$, $\vartheta \in \mathbb{R}^{n_\vartheta}$, $y \in \mathbb{R}^{n_y}$ are state variables, inputs, disturbances, parameters, and outputs of the system, respectively. In Eq. 1, t denotes time, and $f := (f^{dT}, f^{aT})^T$ and h are smooth functions which map from some subset $U \subset \mathbb{R}^{n_x} \times \mathbb{R}^{n_u} \times \mathbb{R}^{n_d} \times \mathbb{R}^{n_\vartheta} \times \mathbb{R}$ into $\mathbb{R}^{n_x}$ and $\mathbb{R}^{n_y}$, respectively. The state variables x and the corresponding equations have been partitioned into dynamic state variables x^d and differential equations f^d, and algebraic variables x^a and equations f^a.

We assert that closed-loop systems can be modeled in the form Eq. 1, if some of the inputs $u(t)$ are replaced by reference signals $r(t)$. This is briefly explained. Assume first that Eq. 1 represents an open-loop system to be augmented by a controller. The controller can be modeled as a nonlinear system itself. In order to distinguish it from the physical system, all symbols referring to the controller are marked with a hat. The inputs of the controller are partitioned into reference signals $\hat{r}(t)$, which, for example, comprise time-dependent set points, and all remaining inputs $\hat{u}(t)$

$$\begin{aligned} \dot{\hat{x}}^d(t) &= \hat{f}^d\left(\hat{x}^d(t), \hat{x}^a(t), \hat{r}(t), \hat{u}(t), \hat{d}(t), \hat{\vartheta}, t\right), \quad \hat{x}^d(0) = \hat{x}_0^d, \\ 0 &= \hat{f}^a\left(\hat{x}^d(t), \hat{x}^a(t), \hat{r}(t), \hat{u}(t), \hat{d}(t), \hat{\vartheta}, t\right) \\ \hat{y}(t) &= \hat{h}\left(\hat{x}^d(t), \hat{x}^a(t), \hat{r}(t), \hat{u}(t), \hat{d}(t), \hat{\vartheta}, t\right) \end{aligned} \tag{2}$$

In the closed-loop system the outputs y of the system are fed to the controller inputs $\hat{u}$, and the controller outputs $\hat{y}$ in turn are fed back to the inputs u of the nonlinear system 5. This yields

$$\begin{aligned} \dot{x}^d(t) &= f^d\left(x^d(t), x^a(t), \hat{y}(t), d(t), \vartheta, t\right), \quad x^d(0) = x_0^d, \\ \dot{\hat{x}}^d(t) &= \hat{f}^d\left(\hat{x}^d(t), \hat{x}^a(t), \hat{r}(t), y(t), \hat{d}(t), \hat{\vartheta}, t\right), \quad \hat{x}^d(0) = \hat{x}_0^d, \\ 0 &= f^a\left(x^d(t), x^a(t), \hat{y}(t), d(t), \vartheta, t\right) \\ 0 &= \hat{f}^a\left(\hat{x}^d(t), \hat{x}^a(t), \hat{r}(t), y(t)\hat{d}(t), \hat{\vartheta}, t\right) \\ 0 &= y(t) - h\left(x^d(t), x^a(t), \hat{y}(t), d(t), \vartheta, t\right) \\ 0 &= \hat{y}(t) - \hat{h}\left(\hat{x}^d(t), \hat{x}^a(t), \hat{r}(t), y(t), \hat{d}(t), \hat{\vartheta}, t\right) \end{aligned} \tag{3}$$

System 3 is of the form of Eq. 1 without output equations, if the replacements $x^d \leftarrow (x^{dT}, \hat{x}^{dT})^T$, $x^a \leftarrow (x^{aT}, \hat{x}^{aT}, y^T, \hat{y}^T)^T$, $f^d \leftarrow (f^{dT}, \hat{f}^{dT})^T$, $f^a \leftarrow (f^{aT}, \hat{f}^{aT}, (y-h)^T, (\hat{y}-\hat{h})^T)^T$, $d \leftarrow (d^T, \hat{d}^T)^T$, $\vartheta \leftarrow (\vartheta^T, \hat{\vartheta}^T)^T$, and $u \leftarrow r$ are made. Note that after closing the loop, the output equations form a system of algebraic equations which will in general no longer explicitly yield y and $\hat{y}$. Thus, the closed-loop system will in general comprise algebraic equations even if the open-loop system and the controller do not.

Since Eq. 1 can be used to model both closed-loop and open-loop systems, we will not distinguish between the two types of systems further.

In order to simplify the notation we will omit the time-dependencies in $x^a(t)$, $x^d(t)$, $u(t)$ and so on. Furthermore, we will assume that the linearization of the algebraic equations f^a in Eq. 1 with respect to x^a have full rank. By virtue of the implicit function theorem (IFT), the algebraic variables can then be expressed as a function of the remaining variables.

$$0 = f^a\left(x^d, x^a, u, d, \vartheta, t\right) \overset{IFT}{\rightarrow} x^a = x^a\left(x^d, u, d, \vartheta, t\right) \tag{4}$$

and the differential-algebraic model is of index one. Substituting Eq. 4 into the nonlinear system (Eq. 1) yields a simplified nonlinear system without algebraic equations

$$\begin{aligned} \dot{x} &= f(x, u, d, \vartheta, t), \quad x(0) = x_0 \\ y &= h(x, u, d, \vartheta, t), \end{aligned} \tag{5}$$

where the label d for the dynamic variables is omitted for simplicity. We will focus on systems of this type (Eq. 5) and defer the discussion of systems with algebraic equations to the appendix.

Having established the terms state variables x, input and reference signals u and r, disturbances d, and parameters ϑ, the restrictions for an application of the approach presented in this article can be stated. Most importantly, we will exclusively address the design of continuous processes operated at steady state. These may either be open-loop or closed-loop processes. In detail we will assume that the following restrictions hold:

(1) Equations f and h in Eq. 5 must not explicitly depend on t.

(2) Inputs $u(t)$ can be partitioned into a constant mean value and bounded time-dependent variations

$$u_i(t) = \bar{u}_i + \eta_{u_i}(t), \quad \eta_{u_i}^{\text{lower}} \le \eta_{u_i}(t) \le \eta_{u_i}^{\text{upper}} \ \forall t \tag{6}$$

Furthermore, the variations are slow compared to the time scales of the system Eq. 5, that is

$$\left| \frac{1}{\eta_{u_i}} \frac{d\eta_{u_i}}{dt} \right| \ll |Re(\lambda_j)|, \forall i, j, \tag{7}$$

where $Re(\lambda_j)$ denote the real parts of the eigenvalues λ_j of the Jacobian of f with respect to x, evaluated at the steady state of interest.

(3) The assumptions on $u(t)$ must also hold for $d(t)$.

(4) In the closed-loop case, the assumptions on $u(t)$ must also hold for $r(t)$.

These assumptions allow us to simplify the notation further. Equations 6 and 7 imply that inputs u, references r, and disturbances d vary only *quasistatically* compared to the system dynamics, and, thus, can be modeled in terms of a mean value and a parametric uncertainty. Parameters ϑ are not time-dependent and can be modeled in the same manner. Note, however, that some of the parameters are typically not uncertain, or the uncertainty can be neglected in the given model. If Eq. 5 models a tank reactor, for example, the volume of the reactor may be a parameter ϑ_i for which the uncertainty can be neglected for all practical purposes. Similarly, there may be inputs u_i for which the uncertainty can be neglected.

The assumptions suggest to repartition inputs, references, disturbances, and parameters into those which are uncertain and those for which uncertainty does not exist or can be neglected. We will, therefore, rewrite the ordinary differential equations of the system (Eq. 5) as

$$\dot{x} = f(x,\alpha,p), \quad x(0) = x_0, \tag{8}$$

$$y = h(x,\alpha,p)$$

where α denotes those inputs u, references r, disturbances d, and parameters ϑ that are modeled in terms of an average value and an uncertainty, while p denotes all inputs, references, disturbances, and parameters for which uncertainty can be neglected. For the lack of a better term, α and p will be referred to as uncertain parameters, and parameters which are not subject to uncertainty, respectively. The output equation does not impact our results, since the outputs y do not enter the state equations. The output equations are, therefore, omitted subsequently.

Nontrivial process optimization problems for systems of the type of Eq. 8 at steady state involve inequality constraints that account for, for example, product quality or safety restrictions. Let α_1 and α_2 in Figure 1 represent uncertain process parameters, and let M^c represent a boundary given by such a constraint. Clearly, in process optimization the nominal point of operation $\alpha^{(0)}$ is required to stay outside of the region bounded by M^c. One approach to process *flexibility* is to ensure that the constraint which corresponds to M^c not only holds for the nominal point, but for all points in some *vicinity of the nominal point*. Let the region bounded by M^r in Figure 1 represent this vicinity of $\alpha^{(0)}$. The size and shape of this region reflects the desired flexibility. If, for a given design, the regions bounded by M^c and M^r in Figure 1 have an empty intersection, the design will be flexible in the sense that process operation will remain feasible even in the presence of the uncertainty described by M^r. It will be shown that stability can be described in terms of a boundary like M^c; thus, the same line of thoughts applies to *stability* boundaries. Note that Figure 1 is incomplete in that more than one boundary M^c may be present, for example, because both a feasibility and a stability boundary have to be taken into account. For simplicity of presentation, we assume first that only one such boundary exists. Multiple constraints are treated further below.

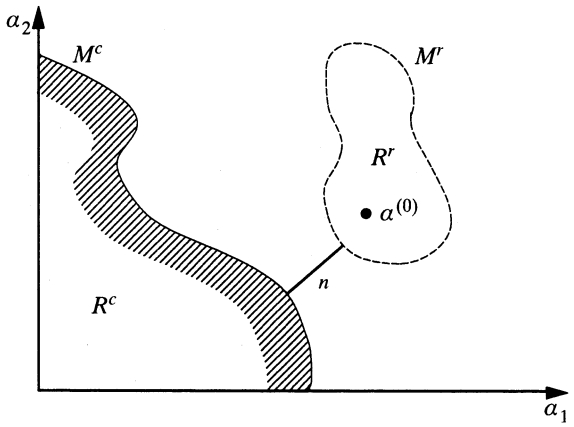

Figure 1. Abstract parametric flexibility problem.

Denoting the regions bounded by M^c and M^r by R^c and R^r, respectively, we can state the process optimization problem with flexibility and parametrically robust stability

$$\begin{aligned} \min_{x,^{(0)}\alpha^{(0)},p^{(0)}} \quad & \phi\left(x^{(0)},\alpha^{(0)},p^{(0)}\right) && \text{(a)} \\ \text{s.t.} \quad & 0 = f\left(x^{(0)},\alpha^{(0)},p^{(0)}\right) && \text{(a)} \\ & \emptyset = R^r\left(\alpha^{(0)},p^{(0)}\right) \cap R^c\left(p^{(0)}\right) && \text{(c)} \\ & x^{(0)} \in X,\ \alpha^{(0)} \in A,\ p^{(0)} \in P. && \text{(d)} \end{aligned} \tag{9}$$

As introduced before, $x \in \mathbb{R}^{n_x}$ are state variables, $\alpha \in \mathbb{R}^{n_\alpha}$ are uncertain parameters, $p \in \mathbb{R}^{n_p}$ are parameters which are not affected by uncertainty, and $X \subset \mathbb{R}^{n_x}$, $A \subset R^{n_\alpha}$, $P \subset \mathbb{R}^{n_p}$ represent simple box constraints on the respective variables and parameters. The upper index zero denotes the nominal point of operation. In particular $\alpha^{(0)}$ are the nominal values of the uncertain parameters. Equation 9b guarantees that the optimal point of operation is a steady state of Eq. 8. Equation 9c guarantees that the regions bounded by M^c and M^r have an empty intersection and, therefore, M^c is not crossed for any value $\alpha \in R^r$. We allow R^r to vary in shape and size when the nominal point $\alpha^{(0)}$ is varied. Similarly, both R^r and R^c may depend on p. We will write $R^r(\alpha,p)$, $R^c(p)$ and, accordingly, $M^r(\alpha,p)$, $M^c(p)$ to point out these dependences where appropriate.

Unified Treatment of Stability and Feasibility

The problem statement (Eq. 9) is preliminary. Obviously, the constraint in Eq. 9c needs further discussion. We will proceed by explaining first how Eq. 9c can be stated for feasibility constraints based on maximizing the constraint violation. After pointing out the difference between feasibility constraints and stability constraints, we show that both can be treated in a unified manner if the notion of the constraint

violation is replaced by the notion of the closest critical points in the space of uncertain parameters.

Assume that a feasibility constraint

$$0 \le g(x,\alpha,p) \tag{10}$$

where g maps into $\mathbb{R}$, has to be enforced for the system (Eq. 8) of interest. The corresponding boundary M^c is given by

$$M^c = \{\alpha \in A,\ x \in X,\ p \in P: 0 = g(x,\alpha,p),\ 0 = f(x,\alpha,p)\} \tag{11}$$

For a constraint of this type, Eq. 9c can be recast in the form

$$0 \le g(x,\alpha,p) \text{ for all } \alpha \in M^r. \tag{12}$$

Existing approaches to process design under uncertainty are based on finding an appropriate sample of values of α which replaces Eq. 12. Such a sample can be identified by maximizing the constraint violation, that is, maximizing g over all steady states $\alpha \in M^r$ for a fixed p. These approaches are based on the assumption that maxima of g correspond to "worst points" in the sense that they violate Eq. 12 with extremal values on the righthand side (Swaney and Grossmann, 1985; Halemane and Grossmann, 1982).

Unfortunately, for stability boundaries a simple condition like Eq. 12 does not exist. The stability of a given steady state could be tested for by calculating the eigenvalues of the linearized process model at a steady-state operating point of interest. If all eigenvalues are in the open left half of the complex plane, the nonlinear process is locally exponentially stable (Hahn, 1967), while the existence of one or more eigenvalues in the open right half of the complex plane implies instability. A calculation of the eigenvalues is tedious, however, in particular if it has to be repeated for a sample of points α which represents Eq. 12. Similarly, identifying the worst points by maximizing real parts of the eigenvalues would be computationally demanding. Kokossis and Floudas (1994) and Mohideen et al. (1997) avoided the tedious calculation of all eigenvalues by using matrix measures. Matrix measures can provide a *single* upper bound for *all* eigenvalues. This bound should, however, not be used, because it is typically not tight and, therefore, may result in an overestimation of the stability boundary at the price of obtaining a suboptimal process design only.

While a simple inequality (Eq. 12) *does not* exist for stability boundaries, a meaningful definition of M^c *does* exist. The stability boundary is characterized by a real eigenvalue or a complex conjugate pair to move from the left half complex plane onto the imaginary axis. However, instead of directly evaluating the eigenvalue criterion, a system of equations implicitly defining M^c can be derived based on bifurcation theory (Dobson, 1993). The technical details of this description will be explained in the section entitled *Stability manifold normal vectors*. At this point, it is sufficient to note that these equations are of the form $0 = g(x,\alpha,p)$ and, therefore, the stability boundary can be described by Eq. 11, that is, in the same manner as a feasibility boundary.

Having obtained a description of the stability boundary, we still need to identify a measure for the parametric robustness of a given steady state with respect to a loss of stability. For this purpose, we determine the parametric distance between the manifolds M^r and M^c. In Figure 1, the closest distance δ between M^c and M^r can be obtained from

$$\begin{aligned} \delta^2 = &\min_{\alpha^c,\alpha^r} n^T n \\ &\text{s.t. } \alpha^c \in M^c \\ &\alpha^r \in M^r \end{aligned} \tag{13}$$

where n is defined as

$$n = \alpha^c - \alpha^r \tag{14}$$

Intuitively, one would like to restate the constraint $R^r \cap R^c = \emptyset$ in Eq. 9 by the requirement that the minimal distance between M^r and M^c is greater than or equal to zero. Obviously, δ as defined in Eq. 13 cannot be used for stating this requirement, as $\delta \ge 0$ by definition. The points marked by dots in Figures 2a and 2b, for example, yield $\delta = 0$, and, therefore, Eq. 13 *does not* allow to distinguish between $R^r \cap R^c = \emptyset$ in Figure 2a and $R^r \cap R^c \neq \emptyset$ in Figure 2b.

We emphasize that the vector (Eq. 14) is a *normal vector* both with respect to manifolds M^c and M^r in Figure 2a. In the section entitled *Relation to minimization of parametric distance*, we discuss how Eq. 13 relates to normal vectors on M^r and M^c, and how normal vectors can be used to replace the constraint $R^r \cap R^c = \emptyset$ in Eq. 9. This can, in fact, be done in a way which retains the intuitive idea of the distance between M^r and M^c of Eq. 13, while avoiding the problem of not being able to distinguish the cases shown in Figure 2.

Normal Spaces to Manifolds

In this section we briefly introduce the notion of a manifold and its tangent and normal space. A basic understanding and a more precise terminology than used before are prerequisites for stating the constraints for robust stability and robust feasibility in the next section.

A nonempty set $M \subset \mathbb{R}^n$ is called a smooth manifold of dimension $n-k$, $k < n$, if, for all points $a \in M$, there exists an open neighborhood $U(a) \subset \mathbb{R}^n$ and k smooth functions

$$\phi_1 : U(a) \to \mathbb{R},\ \ldots,\ \phi_k : U(a) \to \mathbb{R} \tag{15}$$

such that the Jacobian of ϕ with respect to ξ has full rank for all $\xi \in U(a)$ and

$$M \cap U(a) = \{\xi \in U(a) : \phi(\xi) = 0\} \tag{16}$$

For basic notions of differential geometry (in $\mathbb{R}^n$) see, for example, Fleming (1977). For our purposes, it is often suffi-

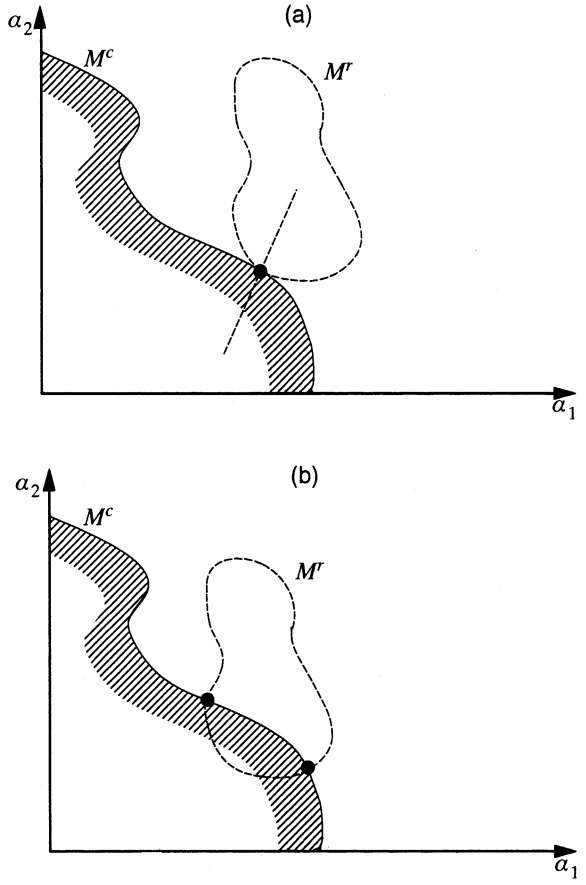

Figure 2. Robustness manifold and critical manifold touch (a) and intersect (b).

The dashed line in (a) marks the common normal direction at the point of intersection of M^r and M^c. At the points in (b) no such common normal direction exists.

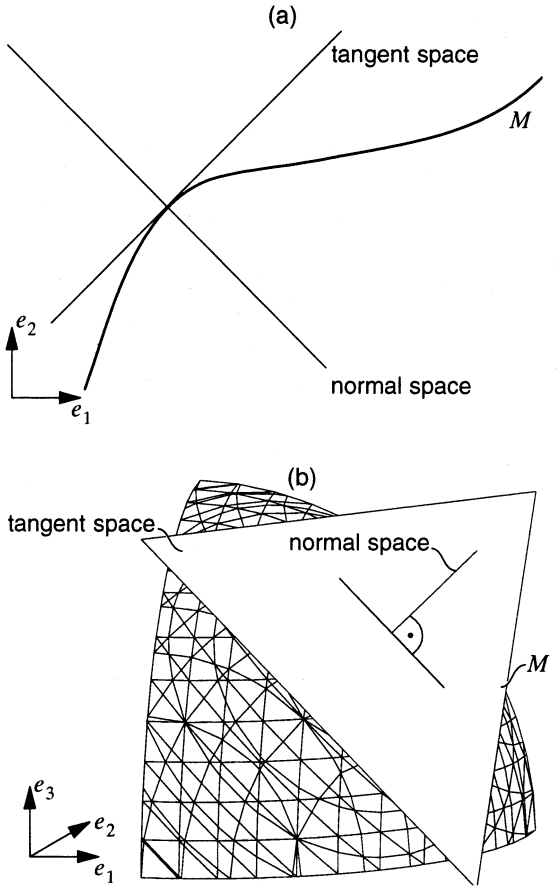

Figure 3. Normal and tangent space for a curve in $\mathbb{R}^2$ and a surface in $\mathbb{R}^3$.

cient and more convenient to describe the manifold in terms of the functions that generate it in $\mathbb{R}^n$. Thus, we let k given smooth functions (Eq. 15) *define* an $(n-k)$-dimensional manifold. This simplifies Eq. 16, since the manifold no longer has to be given in terms of generally different functions on a patchwork of neighborhoods $U(a)$. Equation 16 can be replaced by

$$M = \{\xi \in U : \phi(\xi) = 0\} \tag{17}$$

where $U \subset \mathbb{R}^n$ no longer depends on the point $a \in M$, but is valid for all points on the manifold. Note that M^c, as defined in Eq. 11, is of the form of Eq. 17.

Figure 3 illustrates the dimensions n and k involved in the definition. It is instructive to think of a body to move along the manifolds M in Figure 3. Figure 3a is a sketch in $\mathbb{R}^2$, that is, $n = 2$, with two independent directions to move in. For clarity, let these directions be fixed by two linearly independent unit vectors e_1 and e_2. If we restrict motion by one equation, that is, $k = 1$, this equation will, roughly speaking, fix steps along the unit vector e_2 for a given step along e_1 and vice versa, confining motion to a one-parametric curve, that is, a 1-D manifold $(n - k = 1)$. Similarly, in $\mathbb{R}^3$ spanned by appropriate vectors e_1, e_2, e_3, a single equation will fix the step along one of the unit vectors for given steps along the other two unit vectors, confining motion to a 2-D surface, that is, a 2-D manifold $(n - k = 2)$. Thinking in terms of constraints in optimization again, the 1-D manifold in the $\mathbb{R}^2$ example splits the $\mathbb{R}^2$ into those parts in which the constraint is violated and those parts in which it is inactive. Similarly, the 2-D manifold in the $\mathbb{R}^3$ example splits the $\mathbb{R}^3$ into two such parts.

A basic result from differential geometry states that a linear subspace, the tangent space, can be attached to any point on the manifold locally. As pointed out in the examples above and as expected intuitively, the k equations defining the manifold fix k of the degrees of freedom in $\mathbb{R}^n$, leaving $n - k$ linearly independent directions to move locally tangentially to the manifold. These directions span the $(n-k)$-dimensional tangent space at a given point on the manifold. Again, as expected intuitively, there exist k independent directions in $\mathbb{R}^n$ which are normal to the $n - k$ directions that span the tangent space. Orthogonality is with respect to the usual inner product. Note that tangent and normal spaces are unique, while the directions which span them in general are not.

In the examples given above, the tangent space to the curve in $\mathbb{R}^2$ (that is, to the 1-D manifold in $\mathbb{R}^2$) is 1-D. The normal

space is the 1-D straight line orthogonal to the curve at the respective point. The tangent space of the 2-D surface in $\mathbb{R}^3$ (that is, the 2-D manifold in $\mathbb{R}^3$) is the 2-D plane tangent to the manifold at the point of interest, while the normal space is the straight line normal to the manifold through this point. See Figures 3a and 3b for a sketch.

The notion of a manifold allows us to carry over the concept of a normal space, which we intuitively use in $\mathbb{R}^2$ and $\mathbb{R}^3$ correctly, to higher dimensional spaces. More precisely, letting the k functions in Eq. 15 define an $(n-k)$-dimensional manifold in $\mathbb{R}^n$, the k vectors in $\mathbb{R}^n$

$$b_1 = \nabla\phi_1, \ \ldots, \ b_k = \nabla\phi_k \tag{18}$$

evaluated at a point on the manifold of interest are linearly independent and span the normal space to the manifold at this point (Fleming, 1977). This normal space basis (Eq. 18) will be illustrated with simple examples in the next section.

Flexibility and Robust Stability Constraints

Based on the notions manifold and normal space, constraints can now be stated which allow to recast the requirement $R^r \cap R^c = \emptyset$ (Eq. 9b) into a form that can be implemented. Two details complicate the application of the terms introduced in the previous section. One complication arises because the equations defining the manifolds M^c and M^r involve other variables than uncertain parameters α, namely the state variables x and parameters p. Roughly speaking, we are interested in the normal vector *in the subspace of the uncertain parameters* α, since a measure of the distance between M^c and M^r is needed in this subspace.

The second complication arises because a single feasibility constraint can not always be stated as a single inequality, but an inequality along with an equation or even a set of equations are necessary. A simple example will be given below. Similarly, a constraint for stability cannot be stated as a single equation, but it involves auxiliary equations that determine variables such as eigenvalues or eigenvectors which occur only in the stability constraint, but not in the model or in other constraints. Note that this complication does not result from multiple constraints, but from a single constraint which cannot be stated as a single equation or inequality. Multiple constraints will be treated in the section entitled *Optimization with flexibility and robust stability constraints.*

The present section resolves these complications. For illustrative purposes, a simple model of a continuous fermentation process is introduced.

Illustrative fermentation process example

A simple model for a fermentation process in a CSTR is given by

$$\dot{X} = -\frac{F}{V}X + \mu(S)X \quad = f_1 \tag{19}$$

$$\dot{S} = \frac{F}{V}(S_F - S) - \sigma(S)X = f_2$$

where X [kg m^{-3}] and S [kmol m^{-3}] are the cell concentration and the substrate concentration, F [kg s^{-1}], S_F [kmol m^{-3}], and V [m^3] denote the feed, substrate concentration in the feed and the reactor volume, and $\mu(S) = kS \exp(-S/K)$ [s^{-1}] and $\sigma(S) = \mu(S)/(a + bS)$ [kg kmol^{-1} s^{-1}] are the growth and substrate consumption rate, respectively. In the calculations to follow, we set $k = 1$ m^3 (kmol s)$^{-1}$, $K = 0.12$ kmol m^3, $\alpha = 5.4$ kg kmol^{-1}, $b = 180$ kg m^3 kmol^{-2}, $V = \pi$ (3m)^2 5.7 m. For details on the process model, we refer to Brengel and Seider (1992).

F is replaced by $\bar{F} = F/(10 \text{ kg s}^{-1})$ for better numerical scaling. We assume that S_F and $\bar{F}$ are subject to uncertainty, that is, $\alpha = (\bar{F}, S_F)^T$, furthermore $x = (X, S)^T$. The parameters $p = (k, K, a, b, V)^T$ are assumed to be known precisely in this simple example.

Feasibility boundary normal vectors

For simplicity, it has so far been assumed that a feasibility constraint is given by a single inequality

$$0 \le g(x, \alpha, p), \tag{20}$$

where g maps into $\mathbb{R}$. The corresponding feasibility boundary M^c is defined by the steady states of the process model (Eq. 8) at which this constraint is active

$$M^c = \{(x, \alpha, p) \in U : 0 = g(x, \alpha, p), 0 = f(x, \alpha, p)\}. \tag{21}$$

$U \subset \mathbb{R}^{n_x} \times \mathbb{R}^{n_\alpha} \times \mathbb{R}^{n_p}$ is an appropriate domain for the variables which depends on the process of interest. A larger class of constraints can be accounted for, if we allow the scalar function g to be replaced by a vector-valued function. This type of constraint arises if g depends on intermediate or auxiliary variables $\tilde{x}$, which are not part of the process model, but nevertheless have to be introduced to state the constraint. We first discuss the general form of constraints of this type and give a brief example below. The general form reads

$$\begin{aligned} 0 &= \hat{g}(x, \tilde{x}, \alpha, p) && \text{(a)} \\ 0 &\le g(x, \tilde{x}, \alpha, p) && \text{(b)} \end{aligned} \tag{22}$$

where $\hat{g}$ and g are smooth, defined on some subset $\tilde{U} \subset \mathbb{R}^{n_x} \times \mathbb{R}^{n_{\tilde{x}}} \times \mathbb{R}^{n_\alpha} \times \mathbb{R}^{n_p}$, and map into $\mathbb{R}^{n_{\tilde{x}}}$ and $\mathbb{R}$, respectively. The auxiliary variables are denoted by $\tilde{x} \in \mathbb{R}^{n_{\tilde{x}}}$. Furthermore, the Jacobian of $\hat{g}$ with respect to $\tilde{x}$ is assumed to have full rank. This property will be used below to guarantee that Eq. 22a can be solved for $\tilde{x}$ locally.

The feasibility boundary M^c that corresponds to Eq. 22 is defined by the steady states of the process model (Eq. 8) at which Eq. 22a holds, and at which the inequality (Eq. 22b) is active. Using the abbreviation

$$\begin{aligned} \tilde{g}(x, \tilde{x}, \alpha, p) := \big(&\hat{g}_1(x, \tilde{x}, \alpha, p), \ \ldots, \\ &\hat{g}_{n_{\tilde{x}}}(x, \tilde{x}, \alpha, p), \ g(x, \tilde{x}, \alpha, p)\big)^T \end{aligned} \tag{23}$$

the definition (Eq. 21) of M^c therefore generalizes to

$$M^c = \left\{(x, \tilde{x}, \alpha, p) \in \tilde{U}: 0 = \tilde{g}(x, \tilde{x}, \alpha, p),\ 0 = f(x, \alpha, p)\right\}. \tag{24}$$

It is stressed that $\tilde{g} = (\hat{g}_1, \ldots, \hat{g}_{n_{\tilde{x}}}, g)^T$ comprises $n_{\tilde{x}} + 1$ equations, whereas $\tilde{x}$ has only $n_{\tilde{x}}$ entries. While counter-intuitive at first sight, this can be clarified by counting dimensions. Loosely speaking, the $n_{\tilde{x}} + 1$ equations $0 = \tilde{g}(x, \tilde{x}, \alpha, p)$ in Eq. 24 fix the $n_{\tilde{x}}$ auxiliary variables *as well as* one of the variables x_i of the model. It is instructive to see that this also holds for the case of a single inequality (Eq. 20), and that this case is recovered from the general formulation (Eq. 22) by setting $n_{\tilde{x}} = 0$. In this case, no auxiliary Eq. 22a nor auxiliary variables $\tilde{x}$ exist, and Eq. 22 is reduced to the single inequality (Eq. 22b). Likewise, the set of $n_{\tilde{x}}$ equations $0 = \tilde{g}(x, \tilde{x}, \alpha, p)$ in Eq. 24 is reduced to the single equation $0 = g(x, \alpha, p)$ in Eq. 21. This single equation obviously does not determine any auxiliary variables, but it still fixes *one* of the variables x_i of the model (that is, $n_{\tilde{x}} + 1 = 1$).

Constraints of the type (Eq. 22) arise, for example, if an inequality constraint is a function of outputs y of the process model (Eq. 8). A constraint of the type

$$\begin{aligned} y &= h(x, \alpha, p) \\ 0 &\le g(x, y, \alpha, p) \end{aligned} \tag{25}$$

can be rewritten in the form (Eq. 22) using $\tilde{x} := y$ and $\hat{g}(x, \tilde{x}, \alpha, p) := \tilde{x} - h(x, \alpha, p)$. While Eq. 25 provides explicit formulas for the auxiliary variables $\tilde{x} = y$, the constraint (Eq. 22) is more general in that one may not be able to solve Eq. 22a for the $\tilde{x}$ explicitly. By assumption, Eqs. 22a have full rank with respect to $\tilde{x}$, however. The implicit function theorem, therefore, implies that Eqs. 22 can be solved for the $\tilde{x}$ locally.

Having stated the general form of feasibility constraints (Eqs. 22) and the corresponding definition (Eq. 24) of the critical manifold M^c, normal vectors to M^c can be introduced. We use $\zeta = (x^T, \tilde{x}^T)^T$ and $\phi = (f^T, \tilde{g}^T)^T$ as abbreviations. According to Eq. 18, the normal space to the manifold (Eq. 24) is spanned by

$$b_1 = \begin{pmatrix} \nabla_\zeta \phi_1 \\ \nabla\alpha \phi_1 \end{pmatrix}, \ \ldots, \ b_{n_x + n_{\tilde{x}} + 1} = \begin{pmatrix} \nabla_\zeta \phi_{n_x + n_{\tilde{x}} + 1} \\ \nabla_\alpha \phi_{n_x + n_{\tilde{x}} + 1} \end{pmatrix} \tag{26}$$

evaluated at the point on the manifold of interest. Since we look for the normal vector in the space of the uncertain parameters α, we seek a linear combination in the normal space that does not have a contribution along the variables u. Such a linear combination $k \in \mathbb{R}^{n_x + n_{\tilde{x}} + 1}$ of the vectors (Eq. 26) can be determined from

$$\begin{aligned} \left(\nabla_\zeta \phi_1 | \ldots | \nabla_\zeta \phi_{n_x + n_{\tilde{x}} + 1}\right) k = 0 \qquad & (a) \\ k_0^T k - 1 = 0, \qquad & (b) \end{aligned} \tag{27}$$

where the second equation for some k_0 not normal to k guarantees that the trivial solution $k = 0$ is rejected. The parameter space normal vector n can be evaluated from the remaining rows of the basis vectors (Eq. 26)

$$n = \left(\nabla\alpha \phi_1 | \ldots | \nabla_\alpha \phi_{n_x + n_{\tilde{x}} + 1}\right) k. \tag{28}$$

Mönnigmann and Marquardt (2002a) show that Eqs. 27 and 28 yield a unique normal direction.

As an illustration, we assume that the constraint

$$0 \le 0.7 \text{ kmol m}^{-3} - S_F =: g(S_F) \tag{29}$$

applies in the fermenter example. Since $n_{\tilde{x}} = 0$, we have $\zeta = x = (X, S)^T$ and $\phi = (f^T, g^T)^T$ where f refers to Eq. 19. Equation 27a evaluates to

$$\begin{pmatrix} -\dfrac{\bar{F}}{V} F_0 + \mu(S) & -\sigma(S) & 0 \\ \mu'(S) X & -\dfrac{\bar{F}}{V} F_0 - \sigma'(S) X & 0 \end{pmatrix} \begin{pmatrix} k_1 \\ k_2 \\ k_3 \end{pmatrix} = \begin{pmatrix} 0 \\ 0 \end{pmatrix} \tag{30}$$

which is solved by $k = (0, 0, 1)^T$. This solution is unique apart from a nonzero scaling factor. It obeys Eq. 27b for the choice $k_0 = k$. Evaluating Eq. 28 yields the normal vector

$$n = \begin{pmatrix} -\dfrac{F_0 X}{V} & \dfrac{F_0 (S_F - S)}{V} & 0 \\ 0 & \dfrac{\bar{F} F_0}{V} & -1 \end{pmatrix} \begin{pmatrix} k_1 \\ k_2 \\ k_3 \end{pmatrix} = \begin{pmatrix} 0 \\ -1 \end{pmatrix} \tag{31}$$

Due to the simplicity of Eq. 29, the normal vector is independent of α. This result is visualized in Figure 4 along with less

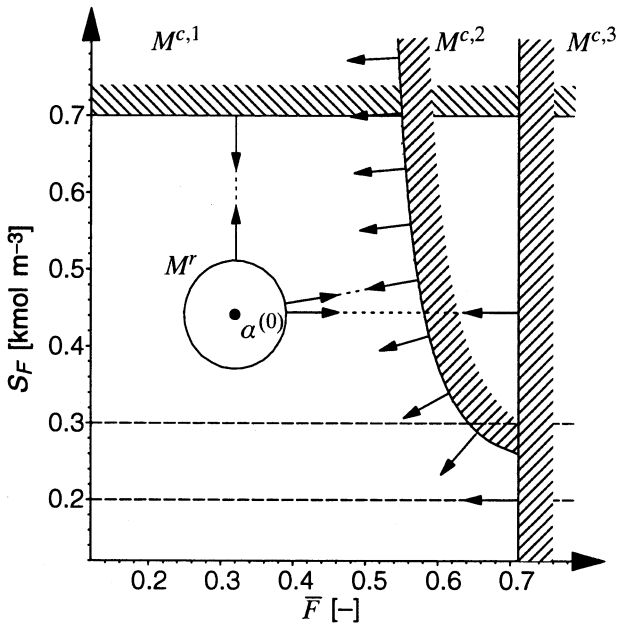

Figure 4. Examples of normal vectors for the fermenter.

$M^{c,1}$ corresponds to the feasibility constraint (Eq. 29). $M^{c,2}$ and $M^{c,3}$ correspond to stability boundaries due to Hopf and saddle-node bifurcations. Figures 5a and 6a are obtained by plotting X along the dashed lines at $S_F = 0.3$ kmol m^{-3} and $S_F = 0.2$ kmol m^{-3}, respectively.

trivial examples of normal vectors to be explained in the next section.

Stability manifold normal vectors

Stability manifold normal vectors will be introduced for process models which consist of ordinary differential equations (ODE) only

$$\dot{x} = f(x, \alpha, p) \tag{32}$$

The extension to models with algebraic equations is deferred to the appendix. The ODE model (Eq. 19) of the fermenter will be used in subsequent illustrations.

The aim of the present section is to describe the loss of stability of an ODE process model by a set of algebraic constraints, which will allow for a characterization of stability boundaries in terms of manifolds of the form (Eq. 17). Note that stability is a property of the dynamical system modeled by differential equations. It is therefore not trivial that a description of stability in terms of algebraic equations exists at all. As explained briefly in the section entitled *Solution approach*, such an algebraic description is possible based on the observation that the existence of an eigenvalue on the imaginary axis is a necessary condition for a loss of stability. Before proceeding to the normal vector systems, this is illustrated further with the fermentation process example (Eq. 19).

Figure 5a shows values of the cell concentration X for equilibria over a range of the dimensionless feed $\bar{F}$ and a fixed value $S_F = 0.3$ kmol m^{-3}. The eigenvalues of the linearized process model evaluated along the points shown in the enlargement are depicted in Figure 5b. The loss of stability occurs when the complex conjugate pair of eigenvalues crosses the imaginary axis. Figures 6a and 6b show similar plots for a fixed substrate feed concentration $S_F = 0.2$ kmol m^{-3}. In this case, the process loses stability as a single real eigenvalue crosses the imaginary axis. The second real eigenvalue is not shown in Figure 6b, since it is well below zero and, therefore, its influence on stability can be neglected.

The illustrated examples correspond to the simplest two cases by which a loss of stability can occur, that is, a single real eigenvalue or a pair of complex conjugate eigenvalues moving from the left half into the right half of the complex plane. The remainder of this section will state the systems of equations which correspond to the existence of a real eigenvalue and a complex conjugate pair on the imaginary axis.

Before proceeding to these systems, we stress that a loss of stability need not occur due to exactly one real eigenvalue or exactly two complex conjugate eigenvalues on the imaginary axis, but may involve any combination of these two basic cases

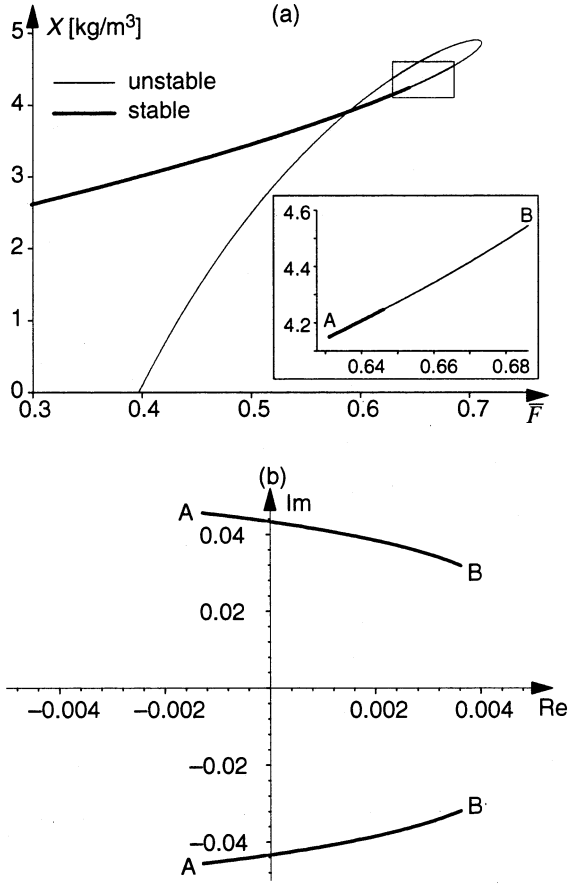

Figure 5. Equilibria of the fermenter for $S_F = 0.3$ kmol m^{-3} (a) and behavior of eigenvalues in the vicinity of the stability boundary (b).

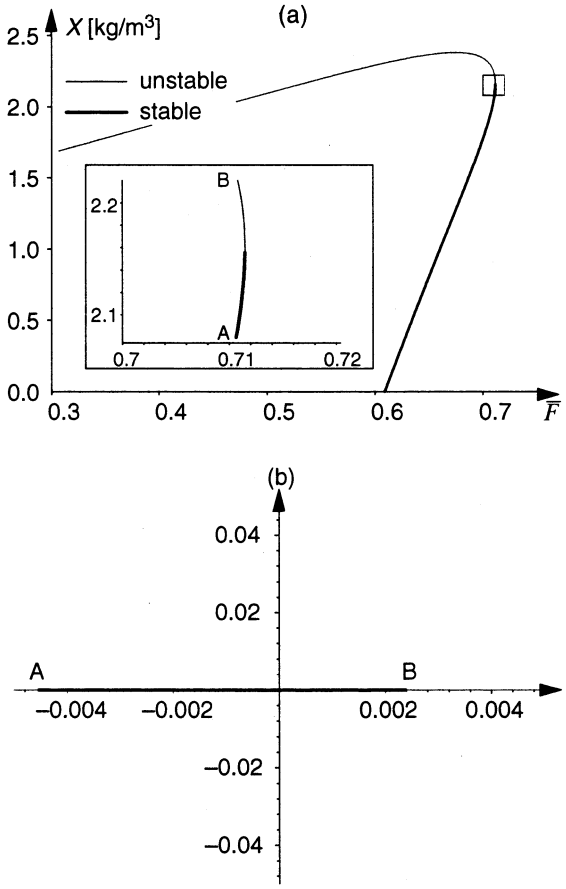

Figure 6. Equilibria of the fermenter for $S_F = 0.2$ kmol m^{-3} (a) and behavior of eigenvalues in the vicinity of the stability boundary (b).

leading to a larger number of eigenvalues on the imaginary axis. For a point to lie on the stability boundary, however, at least a real eigenvalue or a complex conjugate pair of eigenvalues must exist on the imaginary axis. Thus, the systems of equations presented below are necessary conditions for a loss of stability. In fact it is known from bifurcation theory that a loss of stability *typically* occurs due to either exactly one single real, or exactly one complex conjugate pair of eigenvalues on the imaginary axis, and that more complicated situations involving combinations of the two cases rarely occur in physical systems. More precisely, bifurcation theory states that in a n_α-dimensional parameter space, the stability boundary will be given by $(n_\alpha - 1)$-D manifolds of equilibria with either a single real or a complex conjugate pair on the imaginary axis, while combinations of the two basic cases will occur only in the manifolds (or, more generally, sets) of dimensions of at most $n_\alpha - 2$. A thorough discussion of this issue is beyond the scope of this article. For this article, it is important to note that both the detection of stability boundaries and the calculation of normal vectors can be based on the necessary conditions of a single real or a complex conjugate pair of eigenvalues on the imaginary axis presented below. We refer to summarizing articles and textbooks in the bifurcation theory (Guckenheimer and Holmes, 1993; Kuznetsov, 1999; Beyn et al., 2003), and articles which discuss technical details of normal vectors on manifolds of bifurcation points (Dobson, 1993; Mönnigmann and Marquardt, 2002a).

At an equilibrium for which a real eigenvalue on the imaginary axis exists, the system of $2n_x + 1$ equations

$$\left.\begin{aligned} 0 &= f \\ 0 &= f_x^T v \\ 0 &= v^T v - 1 \end{aligned}\right\} \tilde{g} \tag{33}$$

holds. Here f_x^T denotes the transposed Jacobian of the process model (Eq. 32) with respect to x, and $v \in \mathbb{R}^{n_x}$ is the eigenvector corresponding to the eigenvalue zero. Arguments of f and its derivatives are omitted here and in the sequel for brevity. Equations 33 are necessary conditions for a saddle-node bifurcation (Beyn et al., 2003; Kuznetsov, 1999). A 1-D manifold of points which satisfy Eqs. 33 for the fermenter model is given by $M^{c,3}$ in Figure 4.

If a complex conjugate pair of eigenvalues with real part zero exists, the system of $3n_x + 2$ equations

$$\left.\begin{aligned} 0 &= f \\ 0 &= f_x w^{(1)} + \omega w^{(2)} \\ 0 &= f_x w^{(2)} - \omega w^{(1)} \\ 0 &= \overline{w}^T w - 1 \\ 0 &= w^{(1)T} w^{(2)} \end{aligned}\right\} \tilde{g} \tag{34}$$

holds. Again, f_x denotes the Jacobian, $w = w^{(1)} + i w^{(2)}$, $w \in \mathbb{C}^{n_x}$ is the eigenvector of f_x corresponding to the eigenvalue $\lambda = i\omega$, $\omega \in \mathbb{R}$, and $\overline{w}$ denotes the complex conjugate of w. Equations 34 are necessary conditions for a Hopf bifurcation (Beyn et al., 2003; Kuznetsov, 1999). In Figure 4 the 1-D manifold $M^{c,2}$ is composed of points which satisfy Eq. 34.

Equations 33 and 34 are the systems of algebraic equations necessary to state defining equations for the manifolds at which a loss of stability occurs. Substituting Eqs. 33 or 34 into Eq. 24, repeated here for convenience

$$M^c = \left\{ (x, \tilde{x}, \alpha, p) \in \tilde{U} : 0 = \tilde{g}(x, \tilde{x}, \alpha, p),\ 0 = f(x, \alpha, p) \right\}$$

provides a description of the stability manifold which has the same form as the feasibility manifolds in the previous section. Having obtained an algebraic description of the stability boundary, the corresponding normal vector systems can be derived by the line of arguments in Eqs. 26–28. The application of Eqs. 26–28 requires straightforward but tedious linear algebra, thus, we only summarize the resulting normal vector systems and refer to Mönnigmann and Marquardt (2002a) for details.

Using the notation introduced in the previous section, we have $\tilde{x} = v$ for stability boundaries due to a saddle-node bifurcation. In Eqs. 27 and 28, k can be chosen to be $k = (v_1, \ldots, v_n, 0, \ldots, 0)^T \in \mathbb{R}^{2n_x+1}$ (Mönnigmann and Marquardt, 2002a). The $n_x + 1$ trailing zeroes in k allow to reduce the size of the normal vector system considerably (Mönnigmann and Marquardt, 2002a). The resulting system for the normal vector n is given by the $2n_x + n_\alpha + 1$ equations

$$\begin{aligned} &\text{Equations 33} \\ &f_\alpha^T v - n = 0 \end{aligned} \tag{35}$$

For stability boundaries due to a Hopf bifurcation, we have $\tilde{x} = (w_1^{(1)}, \ldots, w_{n_x}^{(1)}, w_1^{(2)}, \ldots, w_{n_x}^{(2)}, \omega)^T \in \mathbb{R}^{2n_x+1}$. Applying Eqs. 26–28 yields $k = (u_1, \ldots, u_n, v_1^{(1)}, \ldots, v_{n_x}^{(1)}, v_1^{(2)}, \ldots, v_{n_x}^{(2)}, 0)^T \in \mathbb{R}^{3n_x+2}$ and the normal vector system

$$\begin{aligned} &\text{Equations 34} \\ f_x^T v^{(1)} - \omega v^{(2)} + \gamma_1 w^{(1)} - \gamma_2 w^{(2)} &= 0 \\ f_x^T v^{(2)} + \omega v^{(1)} + \gamma_1 w^{(1)} + \gamma_2 w^{(2)} &= 0 \\ v^{(1)T} w^{(1)} + v^{(2)T} w^{(2)} - 1 &= 0 \\ v^{(1)T} w^{(2)} - v^{(2)T} w^{(1)} &= 0 \\ f_x^T u + v^{(1)T} f_{xx} w^{(1)} + v^{(2)T} f_{xx} w^{(2)} &= 0 \\ f_\alpha^T u + v^{(1)T} f_{x\alpha} w^{(1)} + v^{(2)T} f_{x\alpha} w^{(2)} - n &= 0 \end{aligned} \tag{36}$$

which consists of $6n_x + 2n_\alpha + 4$ equations. The term $v^{(1)} f_{xx} w^{(1)}$ is short for the tensor product $(v^{(1)} f_{xx}^{w^{(1)}})_i = \sum_{\rho j \sigma} v_\rho^{(1)} \frac{\partial^2 f_s}{\partial x_\sigma \partial x_i} w_\sigma^{(1)}$. The other tensor products in Eqs. 36 are defined accordingly. Note that $v = v^{(1)} + i v^{(2)} \in \mathbb{C}^{n_x}$ can be interpreted as the eigenvector of f_x^T corresponding to the eigenvalue $\overline{\lambda} = -i\omega$. The variables γ_1, γ_2 are auxiliary variables which can be shown to be always zero. They are added to render the normal vector system regular (Mönnigmann and Marquardt, 2002a).

Equations 36 contain second derivatives of f. Adifor (Bischof et al., 1996) and maple (Monagan et al., 2000) are used to calculate these derivatives by automatic and symbolic differentiation in our implementation of the method.

As an illustration, the stability boundary normal vector systems (Eqs. 33 and 35) are evaluated for the fermenter. The

values $X = 2.16$ kg m^{-3}, $S = 0.120$ kmol m^{-3}, $\bar{F} = 0.712$, $S_F = 0.2$ kmol m^{-3} correspond to the equilibrium at which stability is lost in Figure 6. At this point, the Jacobian has an eigenvalue of zero corresponding to the left eigenvector $v = (-1,0)^T$, which satisfies Eq. 33. Equation 35 evaluates to

$$\begin{pmatrix} -\frac{F_0 X}{V} & \frac{F_0(S_F - S)}{V} \\ 0 & \frac{\bar{F}F_0}{V} \end{pmatrix} \begin{pmatrix} -1 \\ 0 \end{pmatrix} - n = 0 \qquad (37)$$

which yields $n = (-0.0134,)^T$. The normal direction defined by this vector is shown in Figure 4.

Normal vectors to M^r

From a technical point of view, normal vectors to the robustness manifold M^r can be calculated in the same manner as normal vectors to feasibility and stability boundaries. M^r differs from feasibility and stability boundaries M^c in that M^r generally varies in form and shape when the nominal point of operation is varied. As explained above, M^r is allowed to vary in shape and location if $\alpha^{(0)}$ is varied (see Figure 1 for an illustration). To account for this variation, the defining equations of M^r may depend on the value of the uncertain parameters at the point of operation $\alpha^{(0)}$. Technically, M^r is parameterized by $\alpha^{(0)}$; thus, $\alpha^{(0)}$ belongs to the parameters p of the defining equations of M^r. The general definition of a manifold M^r here is of the form of Eq. 24, repeated here for convenience

$$M^r = \left\{(x,\tilde{x},\alpha,p) \in \tilde{U} : 0 = \tilde{g}(x,\ \tilde{x},\ \alpha,\ p),\ 0 = f(x,\alpha,p)\right\} \qquad (38)$$

where the smooth functions $\tilde{g}$ map into $\mathbb{R}^{n_{\tilde{x}}+1}$, and $\tilde{U} \subset \mathbb{R}^{n_x} \times \mathbb{R}^{n_{\tilde{x}}} \times \mathbb{R}^{n_\alpha} \times \mathbb{R}^{n_p}$.

Figure 4 illustrates normal vectors on M^r. We assume that the parametric uncertainty of $\bar{F}$ and S_F in the fermenter example can be described by the circle

$$\tilde{g}\left(\bar{F},S_F;\ \bar{F}^{(0)},S_F^{(0)}\right) = \left(\frac{\bar{F} - \bar{F}^{(0)}}{\Delta\bar{F}}\right)^2 + \left(\frac{S_F - S_F^{(0)}}{\Delta S_F}\right)^2 - 2, \quad (39)$$

where $\Delta\bar{F} = 0.05$ and $\Delta S_F = 0.05$ kmol m^{-3}. Since Eq. 39 does not depend on the state variables X and S of the fermenter, the model equations f can be omitted in this case in Eq. 38. Since a single defining equation for M^r remains in this simple example, the normal space is 1-D and the single basis vector can be obtained from Eq. 18 to be

$$n = 2\left(\frac{\bar{F} - \bar{F}^{(0)}}{\Delta\bar{F}^2}, \frac{S_F - S_F^{(0)}}{\Delta S_F^2}\right)^T \qquad (40)$$

Note that this corresponds to evaluating Eq. 28 with $k = k_0 = 1 \in \mathbb{R}$. Figure 4 visualizes normal vectors on M^r for the fermenter example. The direction given by n from Eq. 40 can be interpreted as the direction that is spanned by the line drawn from the center $(\bar{F}^{(0)},\ S_F^{(0)})$ of the circle to any point $(\bar{F},S_F)$ on the circle.

Optimization with Flexibility and Robust Stability Constraints

Having introduced the systems of equations that allow to calculate normal vectors on manifolds M^c and M^r, the nonlinear program (NLP) for the steady-state optimization of continuous processes in the presence of parametric uncertainty can be stated.

In summary, the normal vector systems are nonlinear sets of equations which depend on state variables x of the dynamic system of interest (Eq. 8), on auxiliary variables $\tilde{x}$ such as the eigenvectors in systems for stability boundaries (Eqs. 33 and 34), on the uncertain parameters α, on the parameters not subject to uncertainty p, and, in the case of M^r discussed in the previous section, on the nominal point of operation $\alpha^{(0)}$. In the statement of the NLP below, we will therefore abbreviate the normal vector systems by

$$G^{(t)}\left(x,\tilde{x},\alpha,p,n,\alpha^{(0)}\right) = 0, \quad t \in \{f,s_1,s_2\}, \qquad (41)$$

where the index t denotes the type of manifold. An index $t = f$ refers to feasibility boundaries. In this case, Eq. 41 stands for the defining equations in Eq. 24 and Eqs. 27 and 28. The indices $t = s_1,\ s_2$ denote stability boundaries. In these cases Eq. 41 abbreviates Eqs. 35 and 36, respectively. As pointed out in the previous section, the normal vector system for M^r, denoted by $t = r$, has the same form as the case $t = f$

$$G^{(r)}\left(x,\tilde{x},\alpha,p,n,\alpha^{(0)}\right) = 0. \qquad (42)$$

The optimization problem (Eq. 9) can now be restated using the normal vector systems (Eqs. 41 and 42). As opposed to the introduction of Eq. 9, which focused on the existence of one locally closest critical point for simplicity, more than one locally closest critical point must be accounted for in the general case. Multiple closest connections between M^r and M^c may arise because of multiple constraints, or because of nonconvexity of constraints, cf. Figure 7. Let the upper index $i \in I = \{1,\ \ldots,\ i_{\max}\}$ enumerate critical points $\alpha^{(c,i)}$ and the corresponding points $\alpha^{(r,i)}$ on M^r. For each $i \in I$, the system

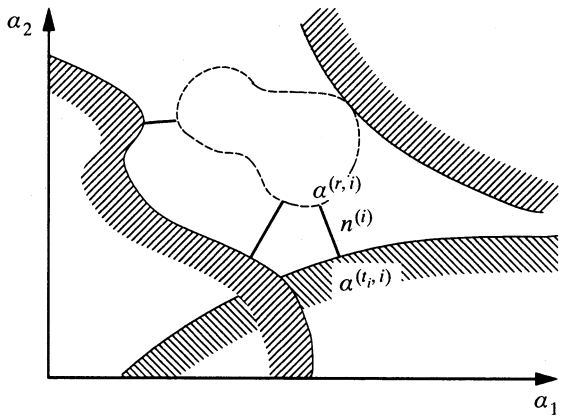

Figure 7. Typically more than one normal vector constraint exists due to the nonconvexity of manifolds M^r, M^c, or because more than one feasibility and stability boundary exist.

of equations

$$0 = G^{(r,i)}\left(x^{(r,i)},\, \tilde{x}^{(r,i)},\, \alpha^{(r,i)},\, p^{(r,i)},\, n^{(i)},\, \alpha^{(0)}\right)$$

$$0 = G^{(t_i,i)}\left(x^{(c,i)},\, \tilde{x}^{(c,i)},\, \alpha^{(c,i)},\, p^{(c,i)},\, n^{(i)},\, \alpha^{(0)}\right)$$

yields the direction $n^{(i)}$ which is normal to the respective manifold at both $\alpha^{(r,i)}$ and $\alpha^{(c,i)}$. Along this normal direction, the distance between $\alpha^{(r,i)}$ and $\alpha^{(c,i)}$ must be equal to or larger than zero. This is ensured by Eq. 46 and the inequality (Eq. 47) in the NLP

$$\min_{x^{(0)},\alpha^{(0)},p^{(0)}} \quad \phi\left(x^{(0)},\alpha^{(0)},p^{(0)}\right) \tag{43}$$

$$\text{s.t.} \quad 0 = f\left(x^{(0)},\alpha^{(0)},p^{(0)}\right), \tag{44}$$

$$0 = G^{(r,i)}\left(x^{(r,i)},\tilde{x}^{(r,i)},\alpha^{(r,i)},p^{(r,i)},n^{(i)},\alpha^{(0)}\right) \tag{45}$$

$$0 = G^{(t_i,i)}\left(x^{(c,i)},\tilde{x}^{(c,i)},\alpha^{(c,i)},p^{(c,i)},n^{(i)},\alpha^{(0)}\right), \quad t_i \in \{f,s_1,s_2\}$$

$$0 = l^{(i)}n^{(i)} - \left(\alpha^{(c,i)} - \alpha^{(r,i)}\right) \tag{46}$$

$$0 \le l^{(i)} \tag{47}$$

$$i \in I,\ x \in X,\ \alpha \in A,\ p \in P \tag{48}$$

which is a restatement of Eq. 9 that can be implemented. Note that $x^{(r,i)}$, $\tilde{x}^{(r,i)}$, $\alpha^{(r,i)}$, $p^{(r,i)}$, $n^{(i)}$,$x^{(c,i)}$, $\tilde{x}^{(c,i)}$, $\alpha^{(c,i)}$, $p^{(c,i)}$, $l^{(i)}$ are degrees of freedom in the optimization in addition to $x^{(0)}$, $\alpha^{(0)}$, $p^{(0)}$. We do not list these variables as arguments of 43 to avoid a too tedious notation.

We will refer to the constraints (Eqs. 45–48) as *minimal distance constraints* for short. Note that this does not mean that we seek a minimal distance, but the name is supposed to reflect that we ensure a distance greater than some acceptable lower bound.

Relation to minimization of parametric distance

The optimization problem (Eq. 13) was used to introduce the notion of parametric distance between candidate points of operation and critical points. With the help of Figure 2, we pointed out that the simple optimization problem (Eq. 13) provides an incomplete characterization of the constraint $R^r \cap R^c = \emptyset$. It is instructive to see why the minimal distance constraints (Eqs. 45–48) avoid the problems of the straightforward measure δ of the distance between the manifolds introduced in Eq. 13.

Using the notation and the abbreviation $\phi = (f^T,\tilde{g}^T)^T$ introduced above, we can rewrite the optimization problem Eq. 13 as

$$\begin{aligned} \delta^2 = \min_{x^r,\alpha^r,x^c,\alpha^c} \ & \frac{1}{2} n^T n \\ \text{s.t.} \quad 0 &= \phi^c\left(x^c,\alpha^c\right) \\ 0 &= \phi^r\left(x^r,\alpha^r\right) \\ 0 &= n - \left(\alpha^c - \alpha^r\right) \end{aligned} \tag{49}$$

where a factor 1/2 has been introduced into the objective as compared to Eq. 13 to simplify the comparison to follow. The first-order Karush-Kuhn-Tucker (KKT) conditions for optimality are $\phi^r = 0$, $\phi^c = 0$ and

$$\begin{aligned} \left(\nabla_{x^r}\phi_1^r|\ldots|\nabla_{x^r}\phi_{n_x n_{\tilde{x}}+1}^r\right)k^r &= 0 \\ -\left(\alpha^c - \alpha^r\right) + \left(\nabla_{\alpha^r}\phi_1^r|\ldots|\nabla_{\alpha^r}\phi_{n_x+n_{\tilde{x}}+1}^r\right)k^r &= 0 \\ \left(\nabla_{x^c}\phi_1^c|\ldots|\nabla_{x^c}\phi_{n_x+n_{\tilde{x}}+1}^c\right)k^c &= 0 \\ \left(\alpha^c - \alpha^r\right) + \left(\nabla_{\alpha^c}\phi_1^c|\ldots|\nabla_{\alpha^c}\phi_{n_x+n_{\tilde{x}}+1}^c\right)k^c &= 0 \end{aligned} \tag{50}$$

where k^r and k^c denote Lagrange multipliers, and arguments of ϕ^r, ϕ^c and their derivatives are omitted for brevity. Comparing the KKT conditions to the normal vector based approach reveals that the first and second rows of equations in Eq. 50 correspond to Eqs. 27a and 28. Thus, $(\alpha^c - \alpha^r)$ in Eq. 50 is a normal vector to M^r. Similarly, the third and fourth rows in Eq. 50 reveal that $(\alpha^c - \alpha^r)$ is a normal vector to M^c. Note, however, that the KKT conditions permit the solution

$$k^r = k^c = 0, \quad n = \left(\alpha^c - \alpha^r\right) = 0 \tag{51}$$

In contrast, the minimal distance constraints reject this type of solution, since a finite length of k is enforced by Eq. 27b. Due to this difference, the minimal distance constraints allow to distinguish between the solutions shown in Figures 2a and 2b while the KKT conditions (Eq. 50) do not. Solutions of the type (Eq. 2a) are accepted by the minimal distance constraints, since the points on M^r and M^c marked by the dot have a common normal direction. Note that a step of length zero, which is accepted by Eq. 47, is necessary along this direction to connect the points on M^r and M^c in Figure 2a. In contrast, the points marked in Figure 2b do not have a common normal direction. While they are solutions of the type (Eq. 51) of the KKT conditions, they are rejected by the minimal distance constraints.

Application to a Continuous Polymerization Process

In this section, the NLP (Eqs. 43–48) is solved for a polymerization reaction carried out in a CSTR. Process models for continuous homopolymerization have been presented, analyzed, and discussed in a series of articles by Ray and coworkers (Schmidt and Ray, 1981; Hamer et al., 1981; Schmidt et al., 1984; Teymour and Ray, 1989, 1992a,b). The process treated here is the solution free radical homopolymerization of vinyl acetate. The stability boundaries for the model are known from a detailed analysis of its nonlinear dynamic behavior (Teymour and Ray, 1992b). Note that the model was derived from a lab-scale reactor model which has been validated experimentally (Teymour and Ray, 1992a). A good summary of the model can be found in DeCicco (2000). We do not repeat the process model, which consists of four differential and 15 algebraic equations, for the sake of brevity.

Optimization problem

We optimize the polymerization of vinyl acetate with respect to the merit function

$$\begin{aligned}\tilde{\Phi}[\text{profit/time}] = &- v_{mf}\rho_{mf}C_m q_{\text{in}} \\ &- v_{sf}\rho_{sf}C_s q_{\text{in}} \\ &- I_f MW_I C_i q_{\text{in}} \\ &+ v_p \rho_p C_p q_{\text{out}},\end{aligned} \tag{52}$$

where v_{mf} and v_{sf} refer to the monomer and solvent volume fraction in the feed, ρ_{mf}, ρ_{sf} and ρ_p are the density of monomer in the feed, solvent in the feed, and polymer in the reactor, MW_{I} and I_f are the molecular weight and the molar concentration of the initiator, θ refers to the residence time, v_p denotes the volume fraction of polymer in the reactor, and the C_i refer to the cost coefficients of the respective substances. The difference between input flow rate q_{in} and output flow rate q_{out} can be neglected. Therefore, we can optimize with respect to the simplified merit function

$$\Phi[\text{profit/time/reactor volume}] = \left(-v_{mf}\rho_{mf}C_m - v_{sf}\rho_{sf}C_s - I_f MW_I C_i + v_p \rho_p C_p\right)/\theta. \tag{53}$$

The optimization results presented below were obtained with the relative cost coefficients $C_m = 3C_s$, $C_p = 6C_m$, $C_i = 20C_p$.

The robustness manifold M^r is chosen to be the ellipsoid defined by

$$g^r(\alpha,\alpha^{(0)}) = \left(\frac{\alpha_1 - \alpha_1^{(0)}}{\Delta\alpha_1}\right)^2 + \left(\frac{\alpha_2 - \alpha_2^{(0)}}{\Delta\alpha_2}\right)^2 - 2, \tag{54}$$

where $\alpha_1 = \theta$, $\alpha_2 = I_f$ and

$$\begin{aligned}\Delta\theta = \Delta\alpha_1 &= 5 \text{ min} \\ \Delta I_f = \Delta\alpha_2 &= 5 \text{ mol/m}^3.\end{aligned} \tag{55}$$

Due to the simplicity of the chosen robustness manifold, the normal vector can be calculated explicitly to be

$$n = 2\left(\frac{\alpha_1 - \alpha_1^{(0)}}{\Delta\alpha_1^2}, \frac{\alpha_2 - \alpha_2^{(0)}}{\Delta\alpha_2^2}\right)^T. \tag{56}$$

This simplifies Eq. 45 considerably.

Results

We will take into account robust stability and flexibility with respect to a temperature restriction. For illustrative purposes, we switch on these constraints one at a time.

For reference, we solve the optimization problem at first without robust stability and flexibility constraints

$$\max_{x^{(0)},\alpha^{(0)}} \phi(x^{(0)},\alpha^{(0)}) \tag{57}$$

$$\text{s.t.} \quad 0 = f(x^{(0)},\alpha^{(0)})$$

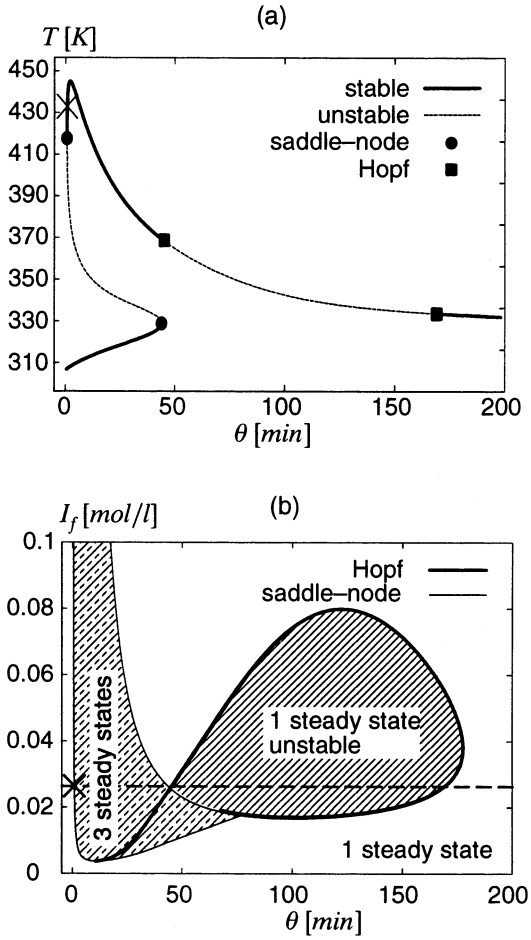

Figure 8. Optimum which results from the NLP (Eq. 57).
The optimum is marked by the cross.

where $\alpha = (\theta, I_f)^T$. The resulting optimal point of operation is $\theta = 0.777$ min, $I_f = 23.4$ mol/m^3, and $T = 430$ K. It is marked by a cross in Figure 8. Figure 8a shows all steady states of the process as a function of θ. Note that multiple steady states exist for θ up to about 50 min. As a rule of thumb, we expect optimal points of operation to be located on the branch of stable steady states at high temperatures, since a high rate of polymer production will occur at high temperature. In Figure 8a, the branch of interest is bounded below with respect to θ by a loss of stability due to a saddle-node bifurcation and bounded above by a loss of stability due to a Hopf bifurcation. Figure 8b shows the location of the stability boundaries which result from saddle-node and Hopf bifurcations as a function of θ and I_f. The particular value of I_f, at which Figure 8a was obtained, is marked by the horizontal dashed line in Figure 8b. Along this line, the points at which stability is lost in Figure 8a can be found. Figure 8 reveals that the process design given by the optimal point marked by the cross cannot be considered robust, as it is parametrically close to a part of the stability boundary which is due to the saddle-node bifurcations.

This result suggests to optimize the process with a minimal distance constraint on the location of the closest saddle-node bifurcation. We, therefore, solve Eqs. 43–48 with $I = \{1\}$ and

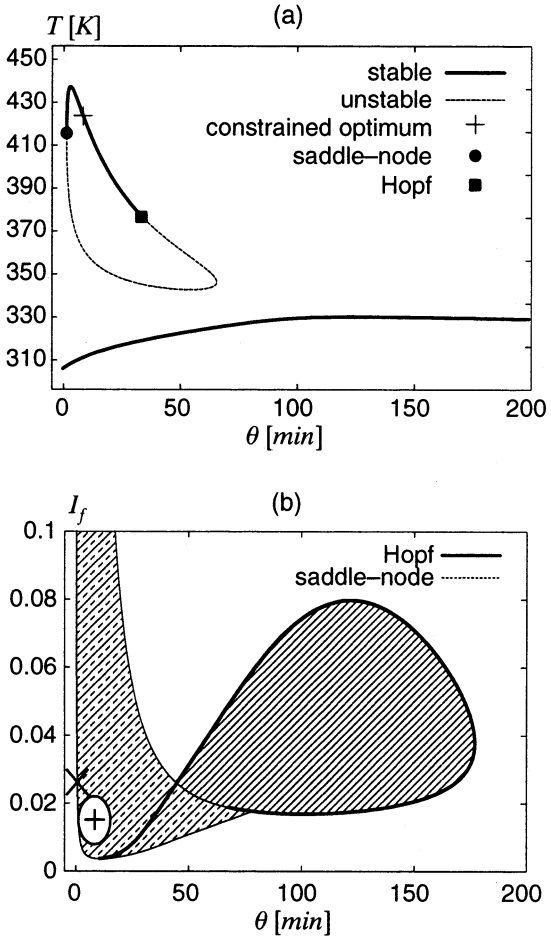

Figure 9. Optimum which results from the optimization with constraint on the minimal distance to the saddle-node bifurcation manifold.

The optimum from Figure 8 is marked for reference.

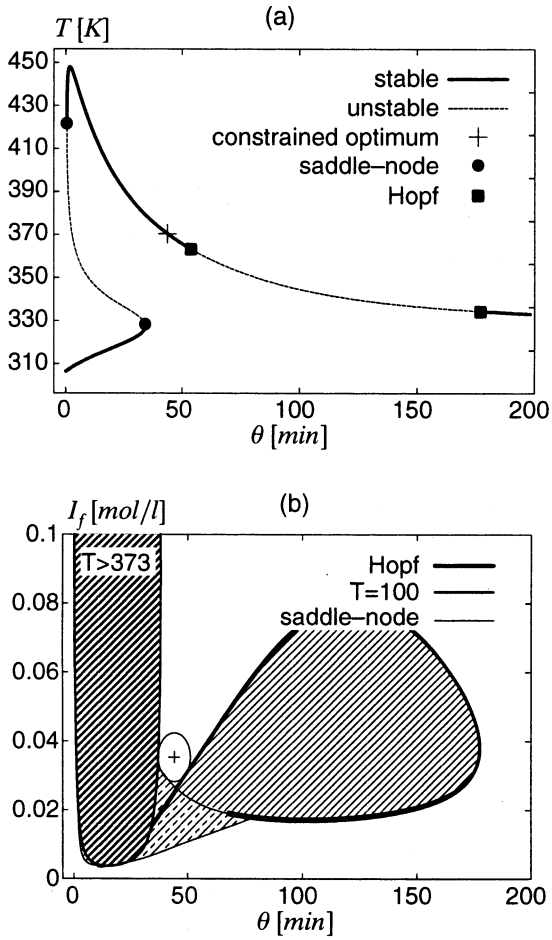

Figure 10. Result of the optimization with constraints on the location of Hopf bifurcations and the temperature constraint $T < 373$K.

$t_1 = s_1$. The result is visualized in Figure 9. A comparison of Figures 8a and 9a shows that the bifurcation diagram changes qualitatively. While a single S-shaped branch of solutions exists in Figure 8a, an isolated branch appears in Figure 9a. We remark that the appearance of closed branches of steady states is due to an isola singularity (Golubitsky and Schaeffer, 1985). The normal vector constraints can deal with this higher codimension singularity without any special adjustments. As opposed to the result in Figure 8, the optimum is now at a safe distance from the stability boundary in Figure 9b. In particular, the process will be stable for any value of the uncertain parameters θ and I_f within the robustness manifold.

In order to demonstrate the use of the normal vector based approach on feasibility boundaries, we impose the temperature constraint $T < 373$ K on the polymerization process in the last optimization problem. The temperature constraint is visualized in Figure 10 along with the stability boundaries. The diagram reveals that the temperature constraint covers up most of the part of the stability boundary which is due to saddle-node bifurcations. In the optimization we, therefore, require the process to be robustly stable with respect to a loss of stability at the remaining Hopf bifurcation manifold and to stay below the temperature constraint for all parameter values in M^r. This amounts to solving Eqs. 43–48 with $I = \{1,2\}$, $t_1 = s_2$, $t_2 = f$. The result is shown in Figure 10. The robustness ellipse in Figure 10b apparently touches the saddle-node bifurcation manifold, but the bifurcation diagram (Figure 10a) reveals that the corresponding saddle-node bifurcations occur on an unrelated part of the equilibrium solution curve, cf. the saddle-node bifurcation at $T \approx 323$ K in Figure 10a.

Table 1 summarizes the values of the merit function (Eq. 53) for the optimization runs. The first column reveals that the merit function drops considerably if the saddle-node distance constraints are imposed. Note that the result for ϕ_{none}

Table 1. Optimization Results*

	$\phi_i/\phi_{\text{none}}$	$\phi_i/\phi_{\text{saddle-node}}$
ϕ_{none}	1	5.0
$\phi_{\text{saddle-node}}$	0.2	1
$\phi_{\text{Hopf,temp}}$	0.03	0.15

*ϕ_{none}, $\phi_{\text{saddle-node}}$, $\phi_{\text{Hopf,temp}}$ refer to the optimization result without minimal distance constraints, with minimal distance constraints on the location of saddle-node bifurcations, and with minimal distance constraints both on Hopf bifurcations and the temperature constraint, respectively.

is of little practical importance, since the process cannot be run at this optimum which is parametrically close to a loss of stability at a saddle-node bifurcation. However, the comparison of ϕ_{none} and $\phi_{\text{saddle-node}}$ reveals that it is an economically reasonable option to stabilize the process in the vicinity of the unconstrained optimum to increase the stability margin by the addition of a controller or by structural design modifications.

Similarly, the merit function value drops considerably, if a temperature constraint is imposed on the process, cf. the second column of Table 1. Again, this result allows to evaluate whether it is economically reasonable to invest into a solvent which is capable of higher temperatures, or to run the process at a lower temperature at the cost of lowering the profit.

Summary and Future Directions

We presented a new approach to the steady-state optimization of continuous processes in the presence of parametric uncertainty. The approach identifies an optimal nominal point of operation which is exponentially stable, and which is feasible with respect to inequality constraints such as physical operating limits or product specifications. Furthermore, the nominal point of operation is guaranteed to be parametrically robust in the sense that stability and feasibility will not be lost despite parametric uncertainty. Although the approach is more general, in the two examples the parametric uncertainty was specified in terms of lower and upper bounds on the uncertain parameters.

The approach is based on enforcing a lower bound on the distance between the optimal point of operation and *critical* points, that is, those points at which feasibility or stability is lost. A unified approach to both feasibility and stability is possible because critical points of either type can be described in terms of manifolds in the space of the uncertain parameters. Normal vectors to these critical manifolds are used to measure the distance to the nominal point of operation. Having identified a measure for the distance between the nominal point of operation and the critical manifolds of the process, constraints can be stated which impose a lower bound on this distance.

The approach presented here differs from existing approaches in that it is not based on the flexibility and feasibility measures proposed by Grossmann and coworkers (Swaney and Grossmann, 1985; Halemane and Grossmann, 1982). As opposed to these measures which evaluate *constraint violation in the range space of the constraints*, we characterize a point of operation by its *distance to the feasibility and stability boundaries in the domain of the uncertain parameters.*. While the concept of constraint violation has been used to address parametrically robust feasibility before, the notion of the distance to critical points in the domain of the uncertain parameters can be applied both to robust feasibility and parametric robustness with respect to stability. Thus, the presented approach allows for a unified treatment of robust feasibility and robust stability.

The normal vector-based constraints were illustrated with a simple fermenter model. Results for the use of the constraints in process optimization with guaranteed parametric robustness and feasibility were shown for a model of the polymerization of vinyl acetate in a CSTR.

In the fermenter and the polymerization example, stability boundaries were known *a priori* since the process models had previously been analyzed with the aid of bifurcation theory and continuation (Agrawal et al., 1982; Teymour and Ray, 1989). In general such an analysis will not be available and, therefore, the set I of all local closest critical points (see Eqs. 43–48) will not be known *a priori*. In fact the proposed normal vector constraints were developed as a first step towards a method which allows to consider stability boundaries, while avoiding a previous bifurcation analysis. In such a method, stability and feasibility boundaries are detected in the optimization instead of conducting the bifurcation analysis by continuation and the optimization separately. While the violation of feasibility boundaries can be detected by simply monitoring the sign of the feasibility constraint along a path of candidate points of operation, special test functions for stability boundaries are necessary. Test functions which signal the crossing of a stability boundary along a path of steady states by a sign change have been used extensively in numerical bifurcation analysis (Beyn et al., 2003). Given an empty or incomplete index set I in Eqs. 43–48, these test functions allow to detect any stability or feasibility boundary which are not yet considered in the current set I as the NLP (Eqs. 43–48) is being solved. If such boundaries are found, the index set can be updated and the optimization problem can be resolved until all boundaries are taken into account. Such an approach is subject to current research.

Literature Cited

Acevedo, J., and E. N. Pistikopoulos, "A Multiparametric Programming Approach for Linear Process Engineering Problems under Uncertainty," *Ind. Eng. Chem. Res.*, **36**, 717 (1997).

Agrawal, P., C. Lee, H. C. Lim, and D. Ramkrishna, "Theoretical Investigations of Dynamic Behavior of Isothermal Continuous Stirred Tank Biological Reactors," *Chem. Eng. Sci.*, **37**, 453 (1982).

Bahri, P. A., J. A. Bandoni, and J. A. Romagnoli, "Effects of Disturbances in Optimizing Control: Steady-State Open-Loop Backoff Problem," *AIChE J.*, **42**(4), 983 (1996).

Bahri, P. A., J. A. Bandoni, and J. A. Romagnoli, "Integrated Flexibility and Controllability Analysis in Design of Chemical Processes," *AIChE J.*, **43**(4), 997 (1997).

Bansal, V., J. Perkins, and E. Pistikopoulos, "Flexibility Analysis and Design of Linear Systems by Parametric Programming," *AIChE J.*, **46**(2), 335 (2000).

Bansal, V., J. D. Perkins, and E. N. Pistikopoulos, "A Unified Framework for the Flexibility Analysis and Design of Non-Linear Systems via Parametric Programming," European Sym. on Computer Aided Process Eng. 11, R. Gani and S. B. Jørgensen, eds., Elsevier Science B. V. (2001).

Beyn, W.-J., A. Champneys, E. Doedel, W. Govaerts, Y. A. Kuznetsov, and B. Sanstede, "Numerical Continuation, and Computation of Normal Forms," *Handbook of Dynamical Systems III: Towards Applications*, B. Fiedler, N. Kopel, and G. Iooss, eds., World Scientific (2003).

Bischof, C., A. Carle, P. Khademi, and A. Mauer, "ADIFOR 2.0: Automatic Differentiation of Fortran 77 Programs," *IEEE Comp. Sc. & Eng.*, **3**(3), 18 (1996).

Brengel, D., and W. Seider, "Coordinated Design and Control Optimization of Non-linear Processes," *Chem. Eng. Comm.*, **16**, 861 (1992).

DeCicco, J., "Simulation of an Industrial Polyvinyl Acetate CSTR and Semibatch Reactor Utilizing MATLAB and SIMULINK: Version 1.0," (2000). Available on the Web at http://www.chee.iit.edu/jdecicco/vinylhtml/VRCTMAN1.html.

Dimitriadis, V. D., and E. N. Pistikopoulos, "Flexibility Analysis of Dynamic Systems," *Ind. Eng. Chem. Res.*, **34**, 4451 (1995).

Dobson, I., "Computing a Closest Bifurcation Instability in Multidimensional Parameter Space," *J. Nonlinear Sci.*, **3**, 307 (1993).
Fleming, W., *Functions of Several Variables*, Springer Verlag, (1977).
Floudas, C. A., Z. H. Gümüş, and M. G. Ierapetritou, "Global Optimization in Design under Uncertainty: Feasibility Test and Flexibility Index Problems," *Ind. Eng. Chem. Res.*, **40**, 4267 (2001).
Golubitsky, M., and D. Schaeffer, *Singularities and Groups in Bifurcation Theory Volume I*, Springer-Verlag, New York (1985).
Grossmann, I. E., and C. A. Floudas, "Active Constraint Strategy for Flexibility Analysis in Chemical Processes," *Comput. Chem. Eng.*, **11**(6), 675 (1987).
Guckenheimer, J., and P. Holmes, *Nonlinear Oscillations, Dynamical Systems, and Bifurcations of Vector Fields*," Springer (1993).
Hahn, W., *Stability of Motion*, Springer Verlag, Berlin (1967).
Halemane, K. P., and I. E. Grossmann, "Optimal Process Design Under Uncertainty," *AIChE J.*, **29**(3), 425 (1982).
Hamer, J. W., T. A. Akramov, and W. H. Ray, "The Dynamic Behaviour of Continuous Polymerization Reactors—II. Nonisothermal Solution Homopolymerization and Copolymerization in a CSTR," *Chem. Eng. Sci.*, **36**, 1897 (1981).
Ierapetritou, M. G., "New Approach for Quantifying Process Feasibility: Convex and 1-d Quasi-Convex Regions," *AIChE J.*, **47**(6), 1407 (2001).
Kabatek, U., and R. E. Swaney, "Worst-Case Identification in Structured Process Systems," *Comput. Chem. Eng.*, **16**, 1063 (1992).
Kokossis, A. C., and C. A. Floudas, "Stability Issues in Process Synthesis," *Comput. Chem. Eng.*, **18**, S93, Suppl. (1994).
Kuznetsov, Y. A., *Elements of Applied Bifurcation Theory*, Springer Verlag, 2nd ed. (1999).
Luyben, M. L., and C. A. Floudas, "Analysing the Interaction of Design and Control—1. A Multiobjective Framework and Application to Binary Distillation Synthesis," *Comput. Chem. Eng.*, **18**(10), 933 (1994).
Mohideen, M., J. Perkins, and E. Pistikopoulos, "Optimal Design of Dynamic Systems under Uncertainty," *AIChE J.*, **42**(8), 2251 (1996).
Mohideen, M., J. Perkins, and E. Pistikopoulos, "Robust Stability Considerations in Optimal Design of Dynamic Systems under Uncertainty," *J. Proc. Cont.*, **7**(5), 371 (1997).
Monagan, M. B., K. O. Geddes, K. M. Heal, G. Labahn, S. M. Vorkoetter, and J. McCarron, *Maple6 Programming Guide*, Waterloo Maple Inc., Waterloo, Canada (2000).
Mönnigmann, M., and W. Marquardt, "Normal Vectors on Manifolds of Critical Points for Parametric Robustness of Equilibrium Solutions of ODE Systems," *J. Nonlinear Sc.*, **12**, 85 (2002a).
Mönnigmann, M., and W. Marquardt, "Parametrically Robust Control-Integrated Design of Nonlinear Systems," *Proc. of American Control Conf.*, Anchorage, AK, Vol. 6, 4321 (2002b).
Ostrovsky, G. M., L. E. K. Achenie, and Y. Wang, "A New Algorithm for Computing Process Flexibility," *Ind. Eng. Chem. Res.*, **39**, 2368 (2000).
Papalexandri, K. P., and T. I. Dimkou, "A Parametric Mixed-Integer Optimization Algorithm for Multiobjective Engineering Problems Involving Discrete Decisions," *Ind. Eng. Chem. Res.*, **37**, 1866 (1998).
Pertsinidis, A., I. E. Grossmann, and G. J. McRae, "Parametric Optimization of MILP Programs and a Framework for the Parametric Optimization of MINLPs," *Comput. Chem. Eng.*, **Suppl.**, S205 (1998).
Pistikopoulos, E. N., "Uncertainty in Process Design and Operations," *Comput. Chem. Eng.* **19**, 553 (1995).
Rooney, W. C., and L. T. Biegler, "Incorporating Joint Confidence Regions into Design under Uncertainty," *Comput. Chem. Eng.*, **23**, 1563 (1999).
Rooney, W. C., and L. T. Biegler, "Design for Model Parameter Uncertainty Using Nonlinear Confidence Regions," *AIChE J.*, **47** (8), 1794 (2001).
Schmidt, A. D., A. B. Clinch, and W. H. Ray, "The Dynamic Behaviour of Continuous Polymerization Reactors—III. An Experimental Study of Multiple Steady States in Solution Polymerization," *Chem. Eng. Sci.*, **39**, 419 (1984).
Schmidt, A. D., and W. H. Ray, "The Dynamic Behaviour of Continuous Polymerization Reactors—I. Isothermal Solution Polymerization in a CSTR," *Chem. Eng. Sci.*, **36**, 1401 (1981).
Swaney, R. E., and I. E. Grossmann, "An Index for Operational Flexibility in Chemical Process Design," *AIChE J.*, **31**(4), 621 (1985).
Teymour, F., and W. H. Ray, "The Dynamic Behaviour of Continuous Polymerization Reactors—IV. Dynamic Stability and Bifurcation Analysis of an Experimental Reactor," *Chem. Eng. Sci.*, **44**, 1967 (1989).
Teymour, F., and W. H. Ray, "The Dynamic Behaviour of Continuous Polymerization Reactors—V. Experimental Investigation of Limit-Cycle Behavior for Vinyl Acetate Polymerization," *Chem. Eng. Sci.*, **47**, 4121 (1992a).
Teymour, F., and W. H. Ray, "The Dynamic Behaviour of Continuous Polymerization Reactors—VI. Complex Dynamics in Full-Scale Reactors," *Chem. Eng. Sci.*, **47**, 4133 (1992b).

Appendix

Stability boundaries of DAE models

In this section we extend normal vector systems for ODE process models to DAE systems of the type

$$\dot{x}^d = f^d\left(x^d, x^a, \alpha, p\right), \quad x^d(0) = x_0^d$$
$$0 = f^a\left(x^d, x^a, \alpha, p\right)$$

where the equations for the outputs y have been omitted because they are not needed in the sequel. In the DAE system, f^d and f^a are considered to be smooth with respect to $x^d \in \mathbb{R}^{n_d}$, $x^a \in \mathbb{R}^{n_a}$, $\alpha \in \mathbb{R}^{n_\alpha}$, $p \in \mathbb{R}^{n_p}$, and the Jacobian of f^a with respect to x^a is assumed to have full rank. According to the implicit function theorem, f^a can be solved for x^a as a function of x^d, α and p. We denote this local solution of x^a as a function of x^d, α and p by $\zeta(x^d, \alpha, p)$. The existence (and smoothness to appropriate order) of $\zeta(x^d, \alpha, p)$ according to the implicit function theorem allows us to investigate the dynamic behavior of the DAE model by considering the ODE system

$$\dot{x}^d = f\left(x^d, \zeta\left(x^d, \alpha, p\right), \alpha, p\right) \tag{A1}$$

making use of

$$0 = f^a\left(x^d, \zeta\left(x^d, \alpha, p\right), \alpha, p\right), \tag{A2}$$

which by continuity holds in some neighborhood of an equilibrium solution of Eq. 5.

Application of the chain rule to Eq. A2 yields the following expressions. Arguments of $f^a(x^d, \zeta(x^d, \alpha, p), \alpha, p)$ and $\zeta(x^d, \alpha, p)$ and of the respective derivatives are omitted for brevity.

For the first derivative of Eq. A2 with respect to x, we have

$$f^a_{x^d} + f^a_{x^a}\zeta_{x^d} = 0$$

where $f^a_{x^d} \in \mathbb{R}^{n_a \times n_d}$, $f^a_{x^a} \in \mathbb{R}^{n_a \times n_a}$, $\zeta_{x^d} \in \mathbb{R}^{n_a \times n_d}$. By assumption, $f^a_{x^a}$ has full rank. Thus, after inverting $f^a_{x^a}$, ζ_{x^d} can be determined from

$$\zeta_{x^d} = -f^{a-1}_{x^a} f^a_{x^d} \tag{A3}$$

For the first derivative of Eq. A2 with respect to α, we have

$$f^a_{x^a}\zeta_\alpha + f^a_\alpha = 0$$

and ζ_α can be obtained from

$$\zeta_\alpha = -f^{a\,-1}_{x^a} f^a_\alpha \tag{A4}$$

For second derivatives of Eq. A2 with respect to x, we find

$$f^a_{x^d x^d} + 2f^a_{x^d x^a}\zeta_{x^d} + f^a_{x^a x^a}\zeta_{x^d}\zeta_{x^d} + f^a_{x^a}\zeta_{x^d x^d} = 0$$

Thus, $\zeta_{x^d x^d}$ can be determined from

$$\zeta_{x^d x^d} = -f^{a\,-1}_{x^a}\left(f^a_{x^d x^d} + 2f^a_{x^d x^a}\zeta_{x^d} + f^a_{x^a x^a}\zeta_{x^d}\zeta_{x^d}\right) \tag{A5}$$

For the mixed derivatives of Eq. A2 with respect to x, α we find

$$f^a_{x^d x^a}\zeta_\alpha + f^a_{x^d\alpha} + f^a_{x^a x^a}\zeta_{x^d}\zeta_\alpha + f^a_{x^a\alpha}\zeta_{x^d} + f^a_{x^a}\zeta_{x^d\alpha} = 0$$

and $\zeta_{x^d\alpha}$ can be determind from

$$\zeta_{x^d\alpha} = -f^{a\,-1}_{x^a}\left(f^a_{x^d x^a}\zeta_\alpha + f^a_{x^d\alpha} + f^a_{x^d\alpha}\zeta_{x^d}\zeta_\alpha + f^a_{x^a\alpha}\zeta\right) \tag{A6}$$

In summary, ζ_x, ζ_α, ζ_{xx} and $\zeta_{x\alpha}$ can be determined from Eqs. A3–A6 by matrix vector multiplications after the inversion of the $n_a \times n_a$-matrix $f^a_{x^a}$.

The derivatives of f which occur in the normal vector systems 35 and 36 can now be calculated. By applying the chain rule to

$$0 = f^d\left(x^d, \zeta\left(x^d, \alpha, p\right)\alpha, p\right) \tag{A7}$$

the same expressions are obtained as for Eq. A2. In the normal vector systems 35 and 36, the replacements

$$\begin{aligned}
f_x &\leftarrow f^d_{x^d} + f^d_{x^a}\zeta_{x^d}\\
f_\alpha &\leftarrow f^d_{x^a}\zeta_\alpha + f^d_\alpha\\
f_{xx} &\leftarrow f^d_{x^d x^d} + 2f^d_{x^d x^a}\zeta_{x^d} + f^d_{x^a x^a}\zeta_{x^d}\zeta_{x^d} + f^d_{x^a}\zeta_{x^d x^d}\\
f_{x\alpha} &\leftarrow f^d_{x^d x^a}\zeta_\alpha + f^d_{x^d\alpha} + f^d_{x^a x^a}\zeta_{x^d}\zeta_\alpha + f^d_{x^a\alpha}\zeta_{x^d} + f^d_{x^a}\zeta_{x^d\alpha}
\end{aligned} \tag{A8}$$

are needed using the results for ζ_x, ζ_α, ζ_{xx} and $\zeta_{x\alpha}$ obtained from Eqs. A3–A6 and its derivatives to account for the algebraic equations in the DAE process model 5.

Manuscript received Jan. 3, 2002, revision received Mar. 5, 2003, and final revision received Aug. 11, 2003.